Supporting information

SI.1 HPLC control of the enantiomeric purity of the antipodes of compound 1

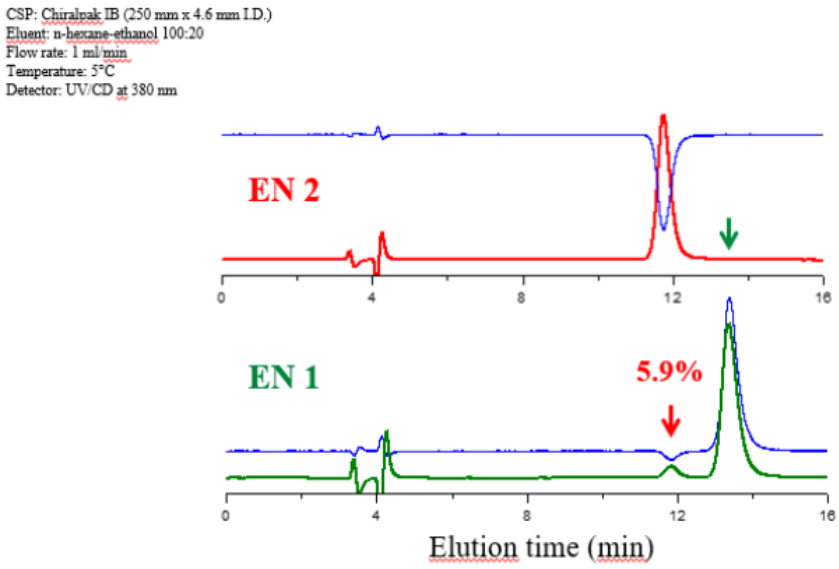

SI.2 CD spectra of the antipodes of monomers 2 and 3, recorded in CH_2Cl_2

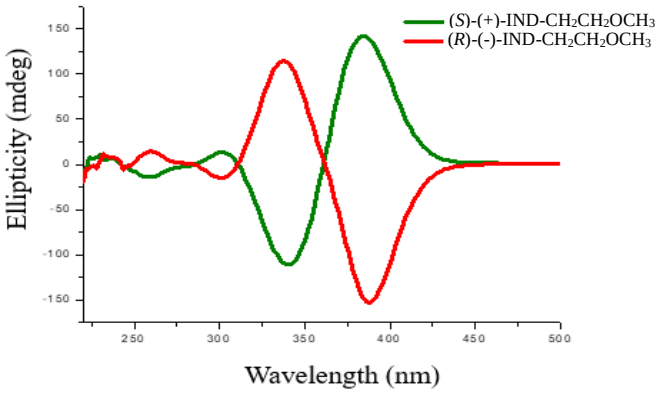

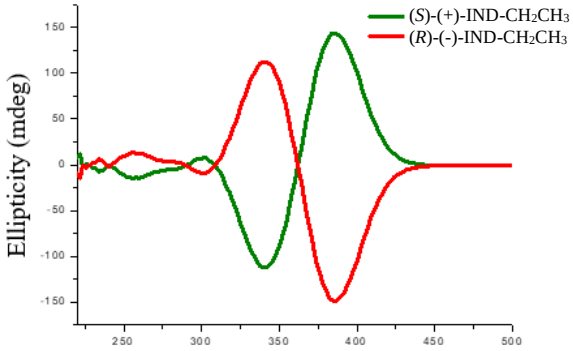

SI.3 ^{1}H and ^{13}C NMR spectra of unknown compounds

SI.3.1: ^{1}H NMR spectrum of (S_{ax},1*R*,2*S*,5*R*)-5

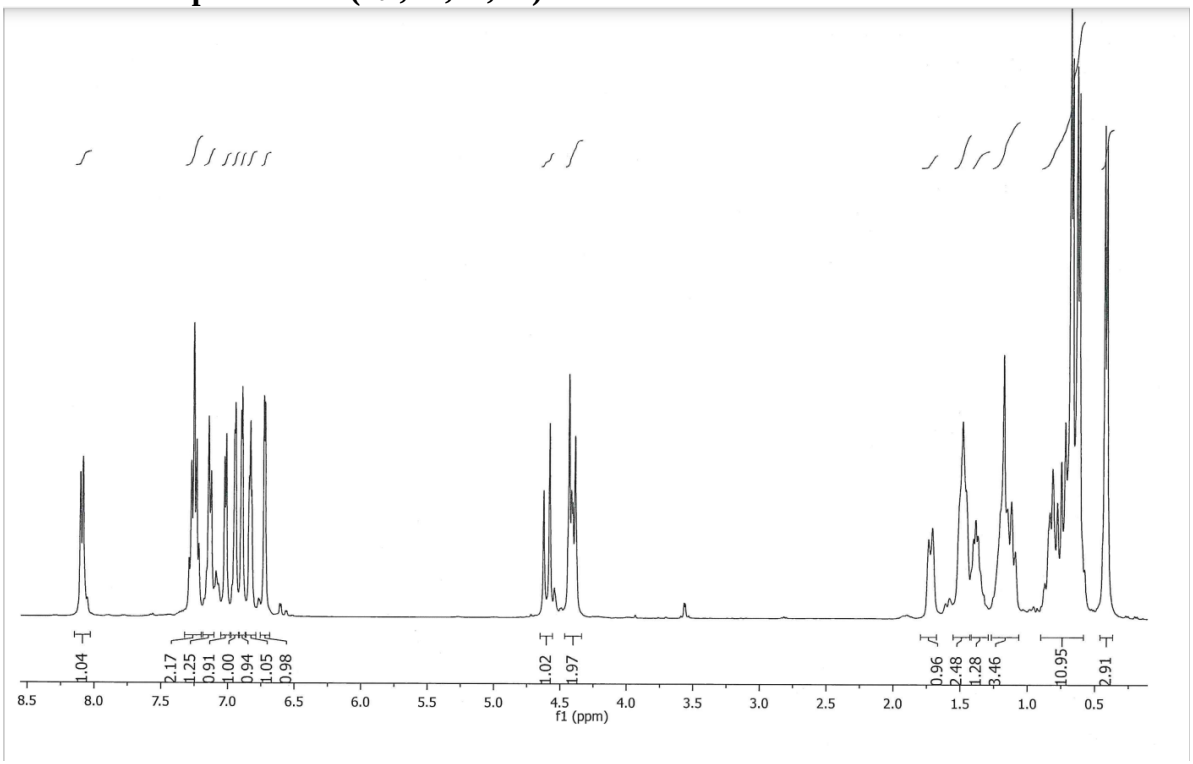

SI.3.2: ^{13}C NMR spectrum of (S_{ax},1*R*,2*S*,5*R*)-5

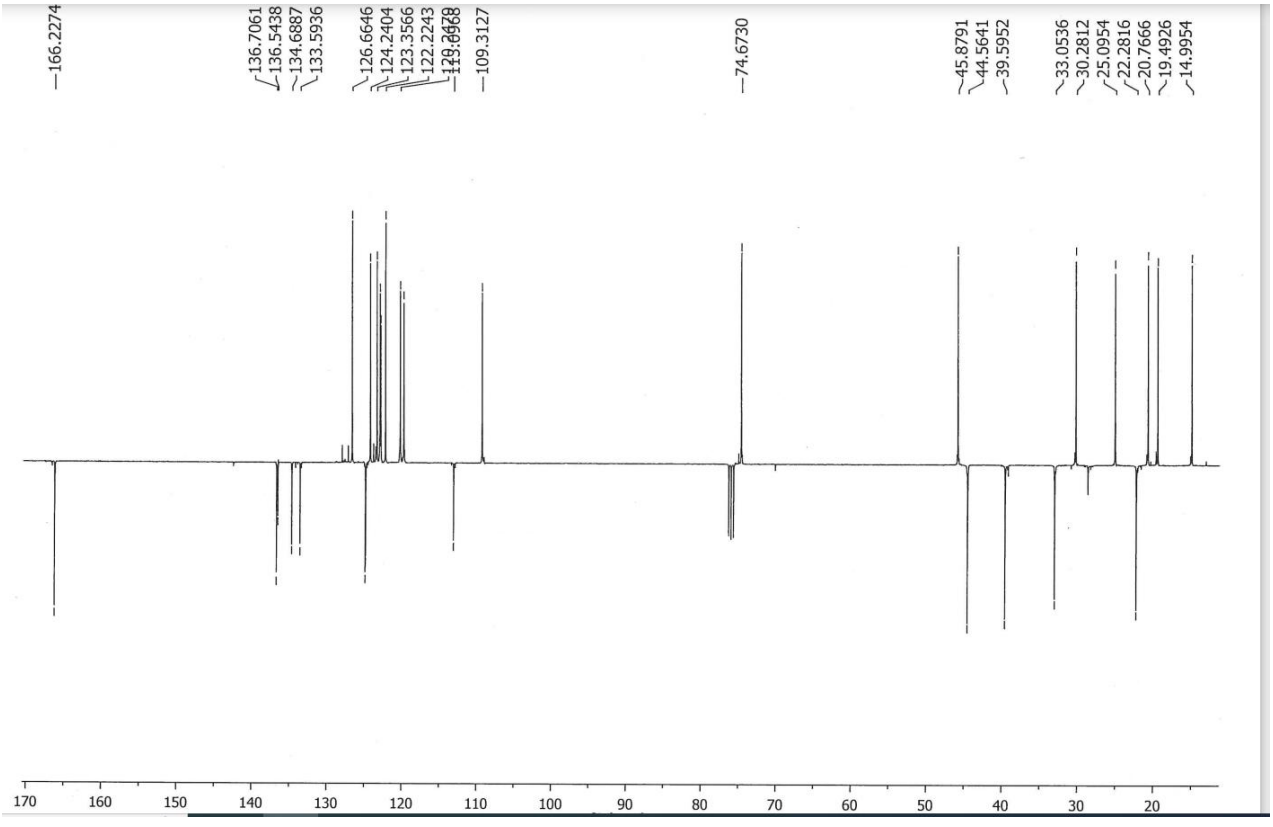

SI.3.3: ^{1}H NMR spectrum of (*R*ax,1*R*,2*S*,5*R*)-5

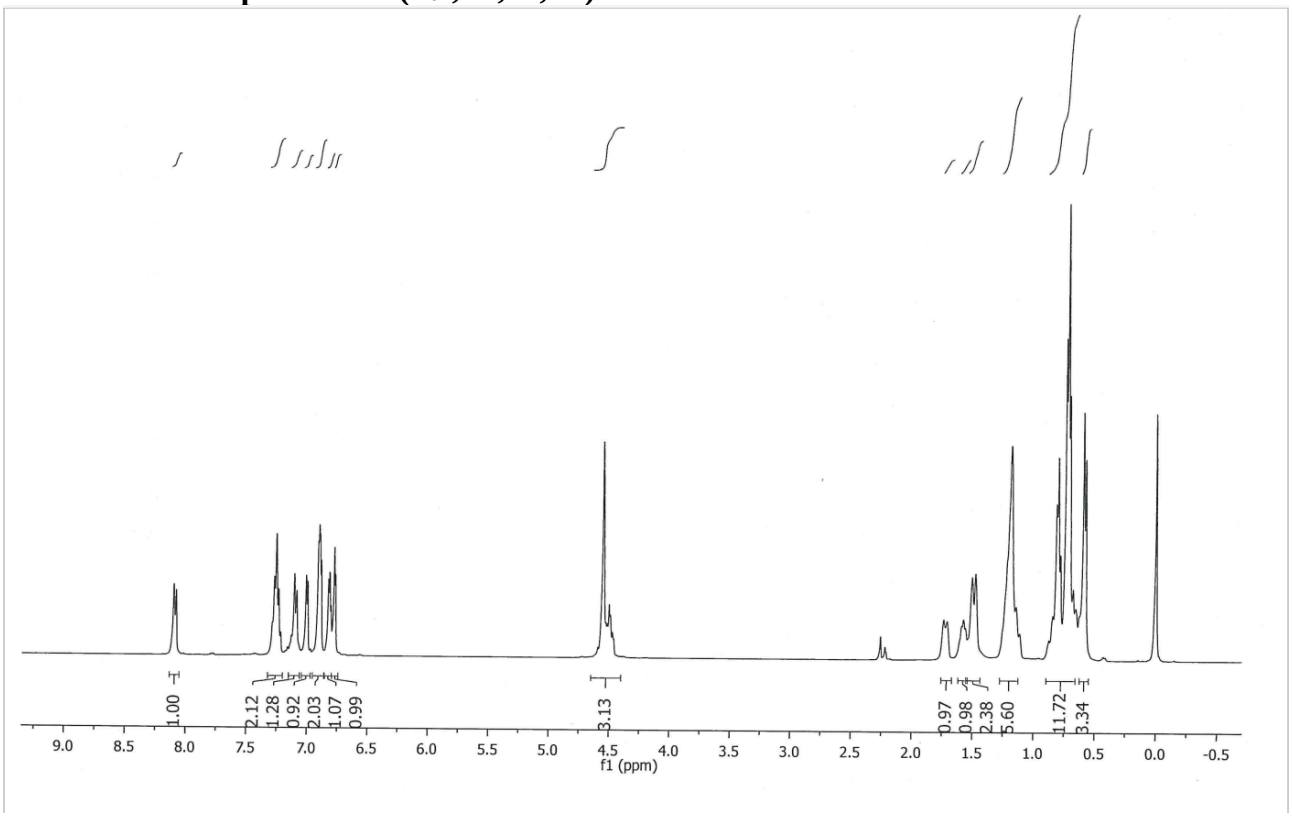

SI.3.4: ^{13}C NMR spectrum of (*R*ax,1*R*,2*S*,5*R*)-5

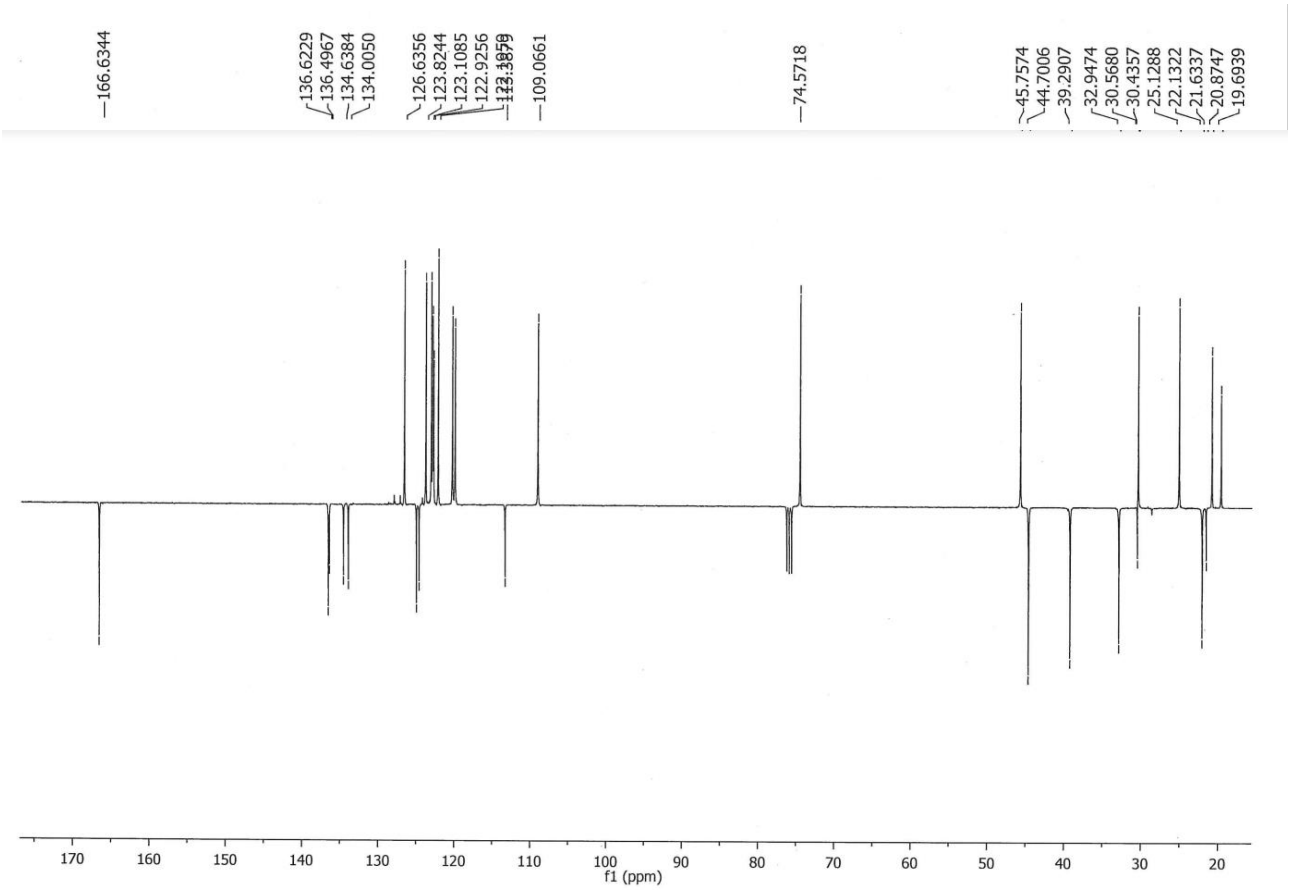

SI.3.5: ^{1}H NMR spectrum of IND-CH_2CH_2OH

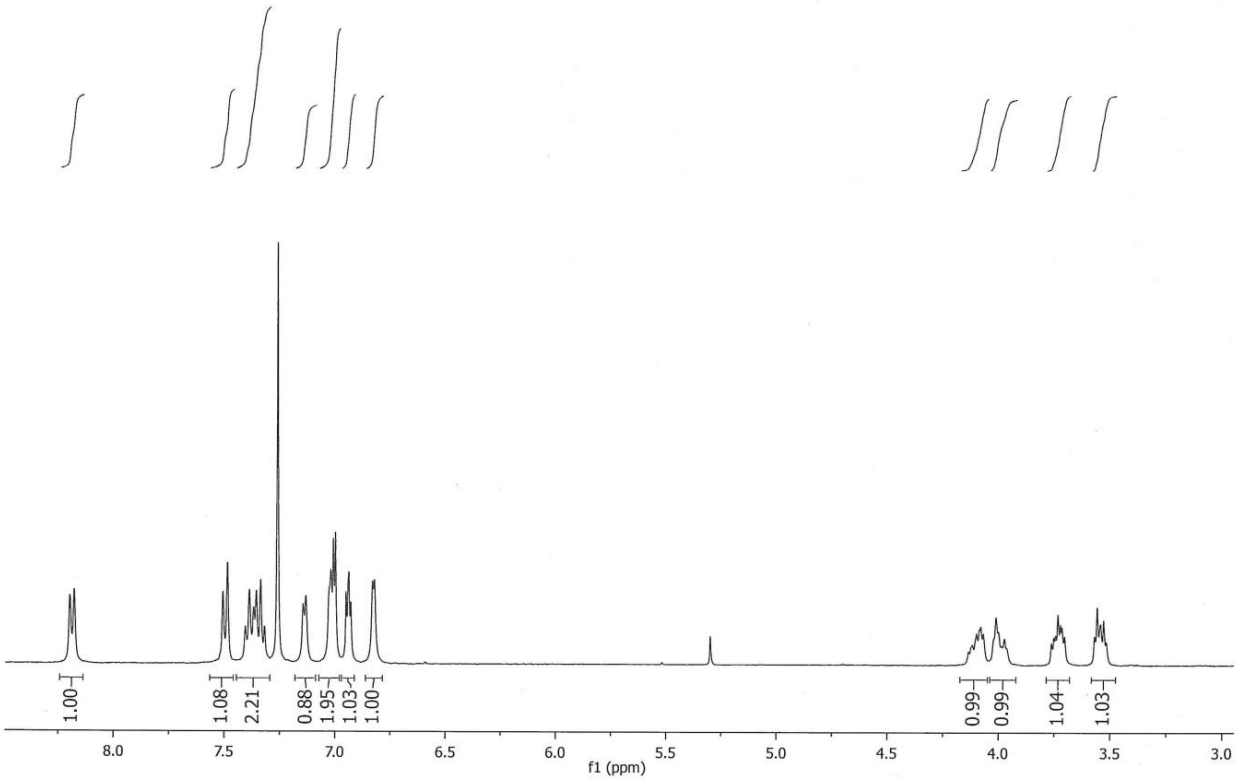

SI.3.6: ^{13}C NMR spectrum of IND-CH_2CH_2OH

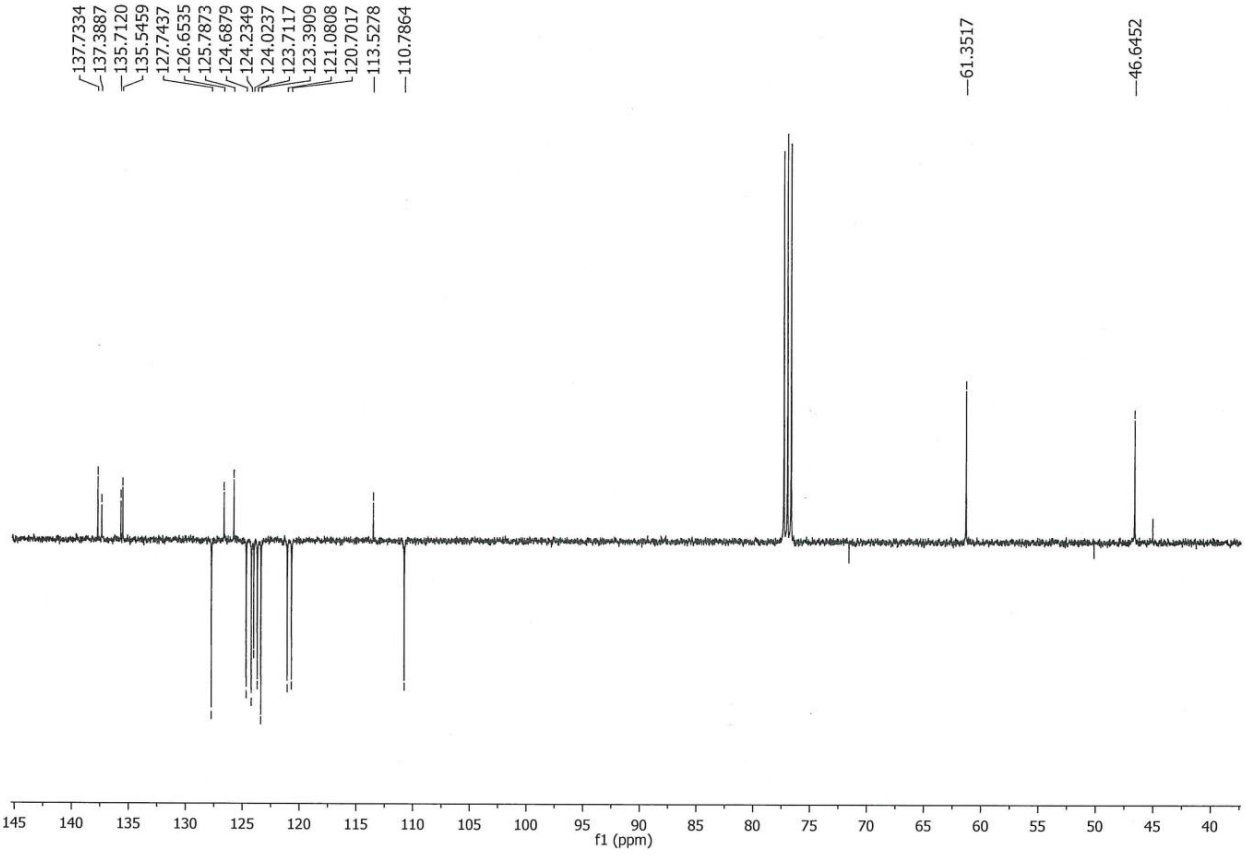

SI.3.7: ^{1}H NMR spectrum of IND-$CH_2CH_2OCH_3$

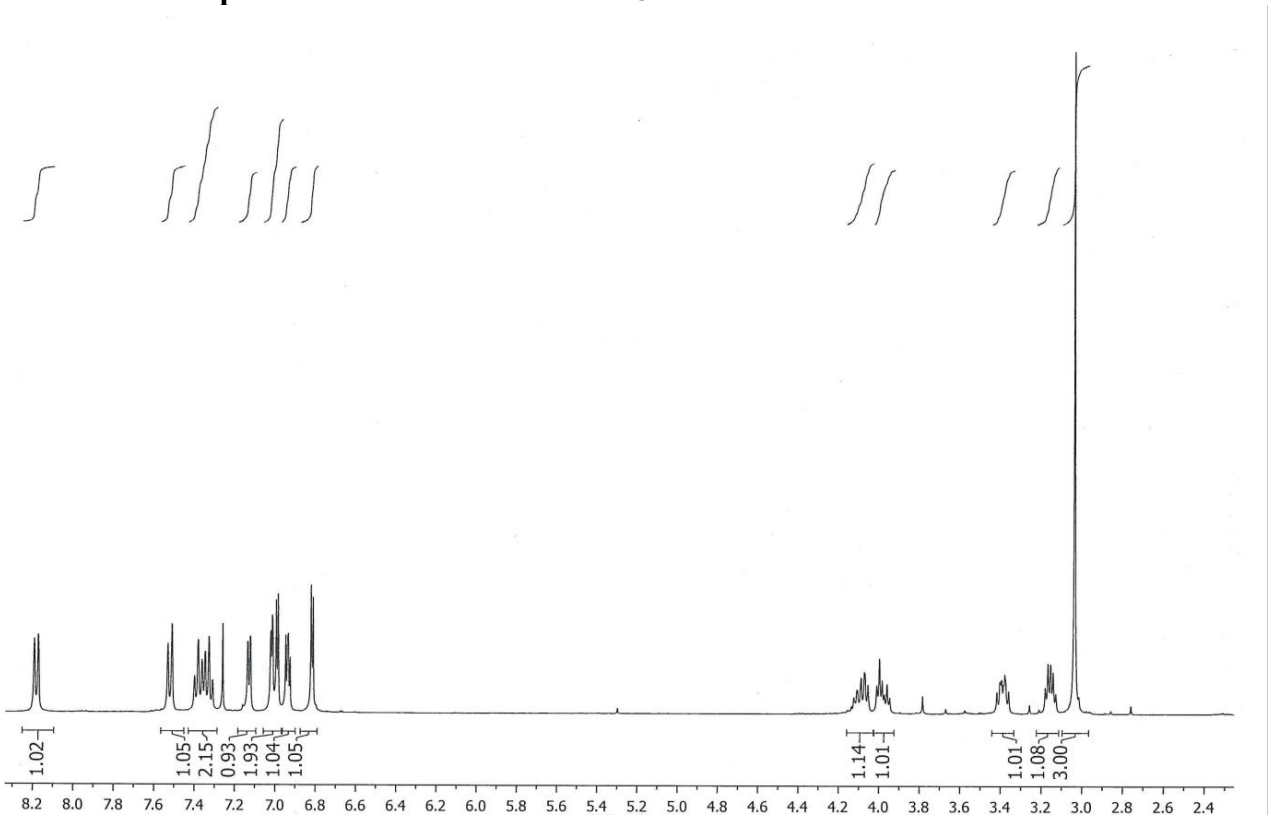

SI.3.8: ^{13}C NMR spectrum of IND-$CH_2CH_2OCH_3$

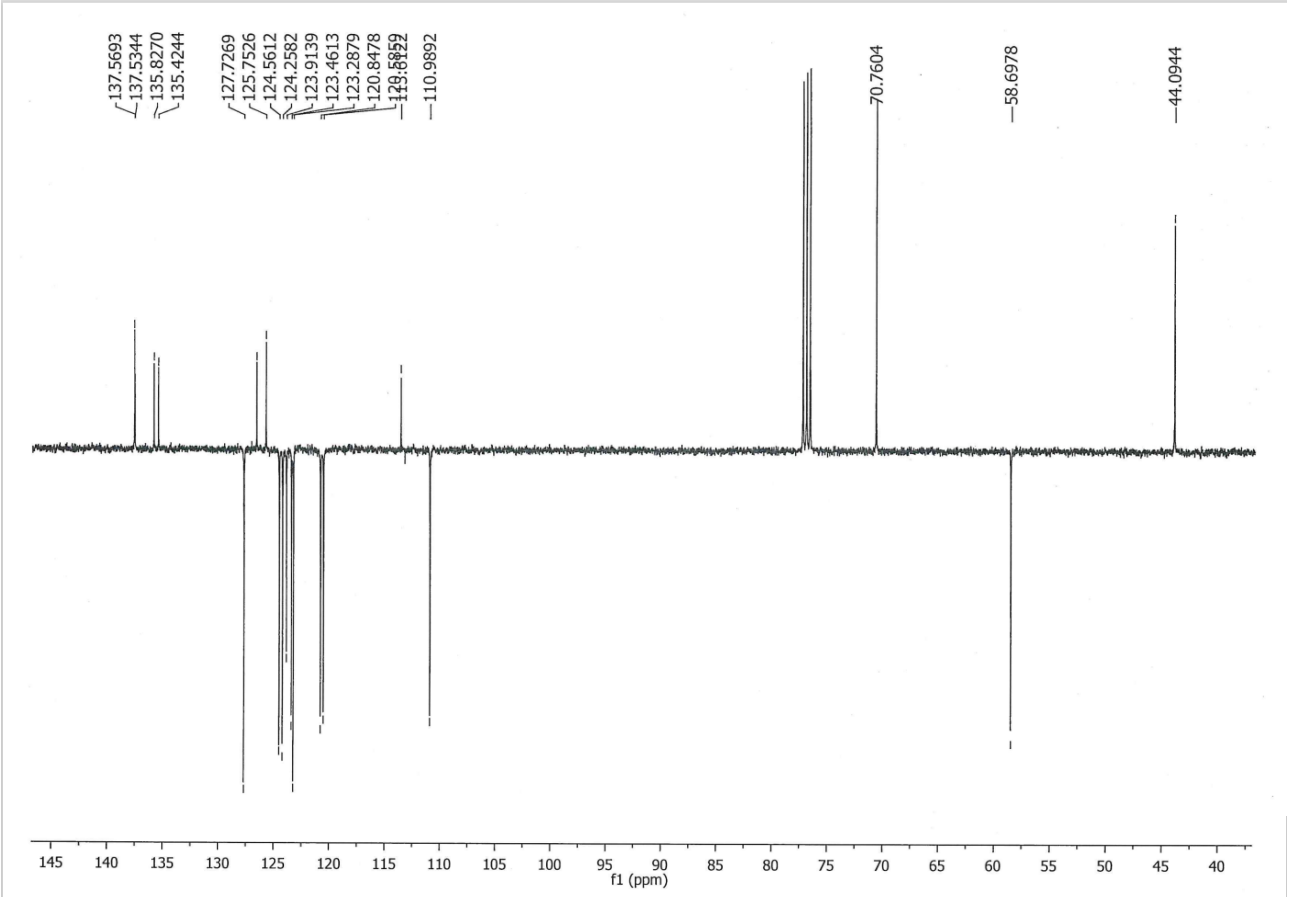

SI.3.9: ^{1}H NMR spectrum of 6

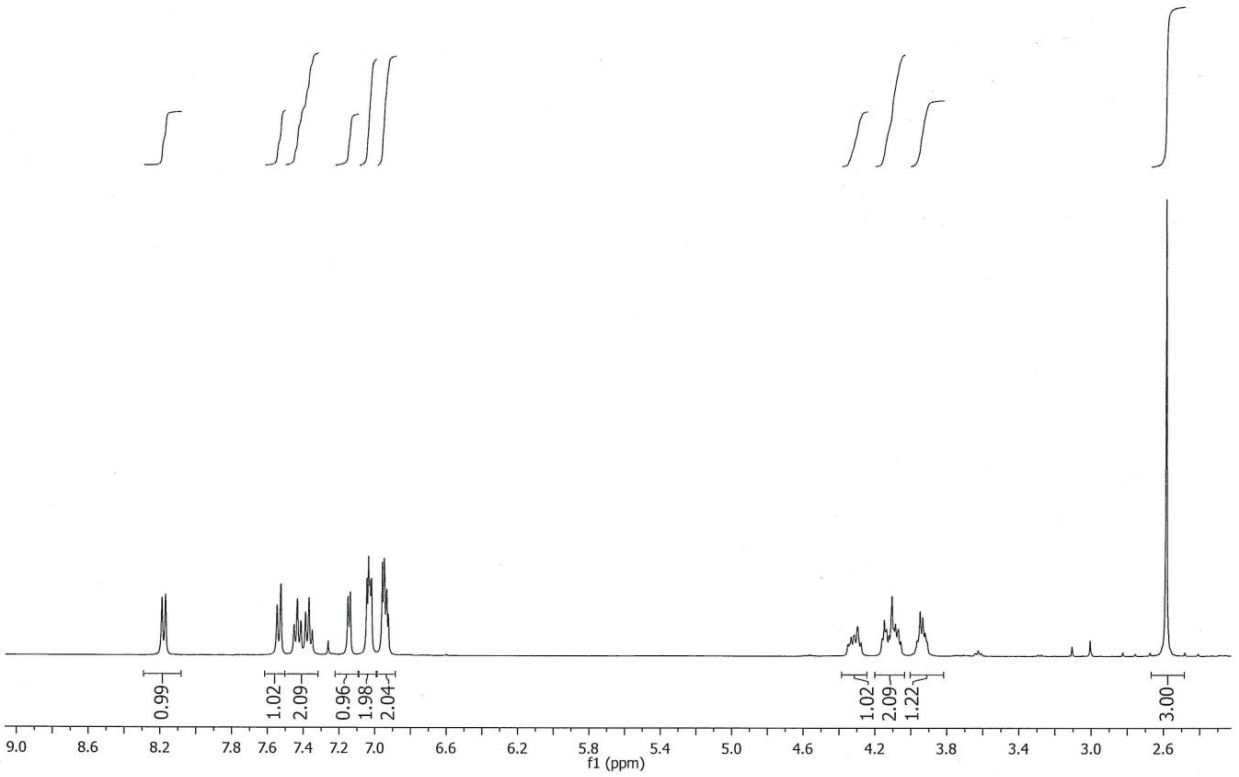

SI.3.10: ^{13}C NMR spectrum of 6

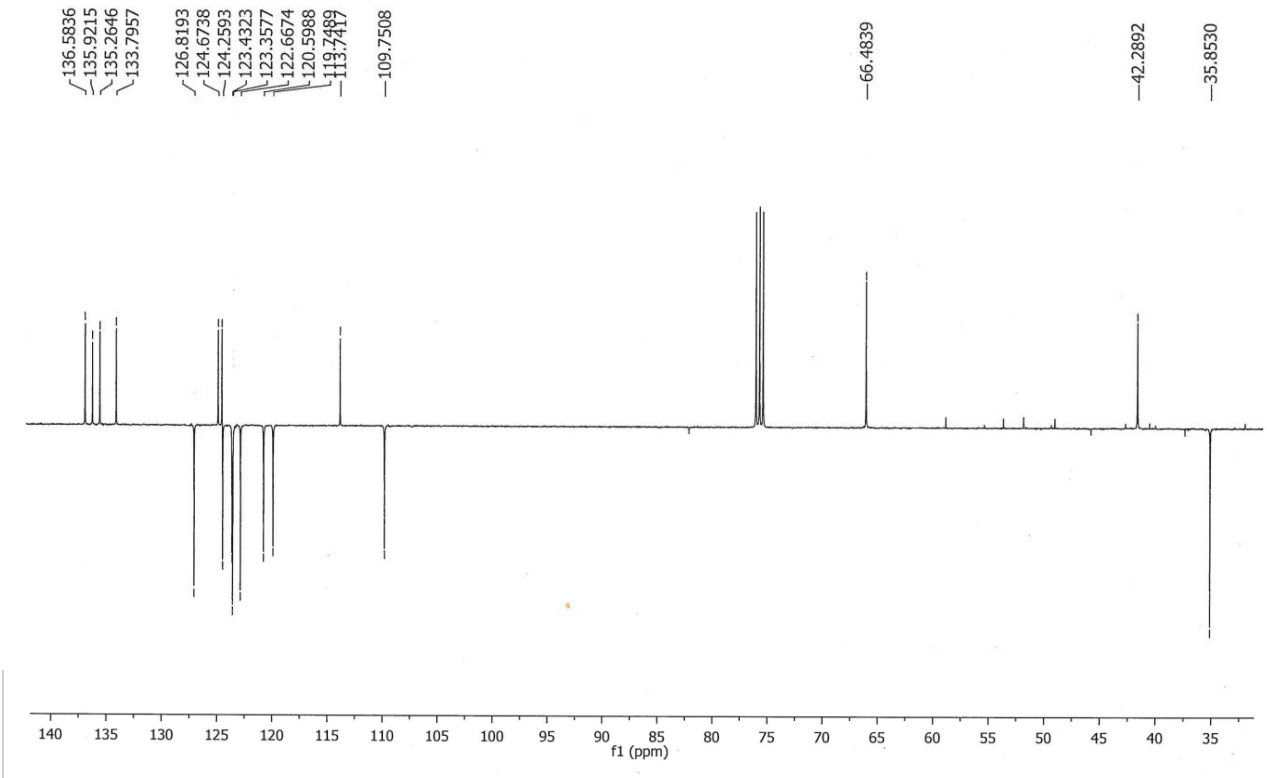

SI.3.11: ^{1}H NMR spectrum of IND-CH_2CH_3

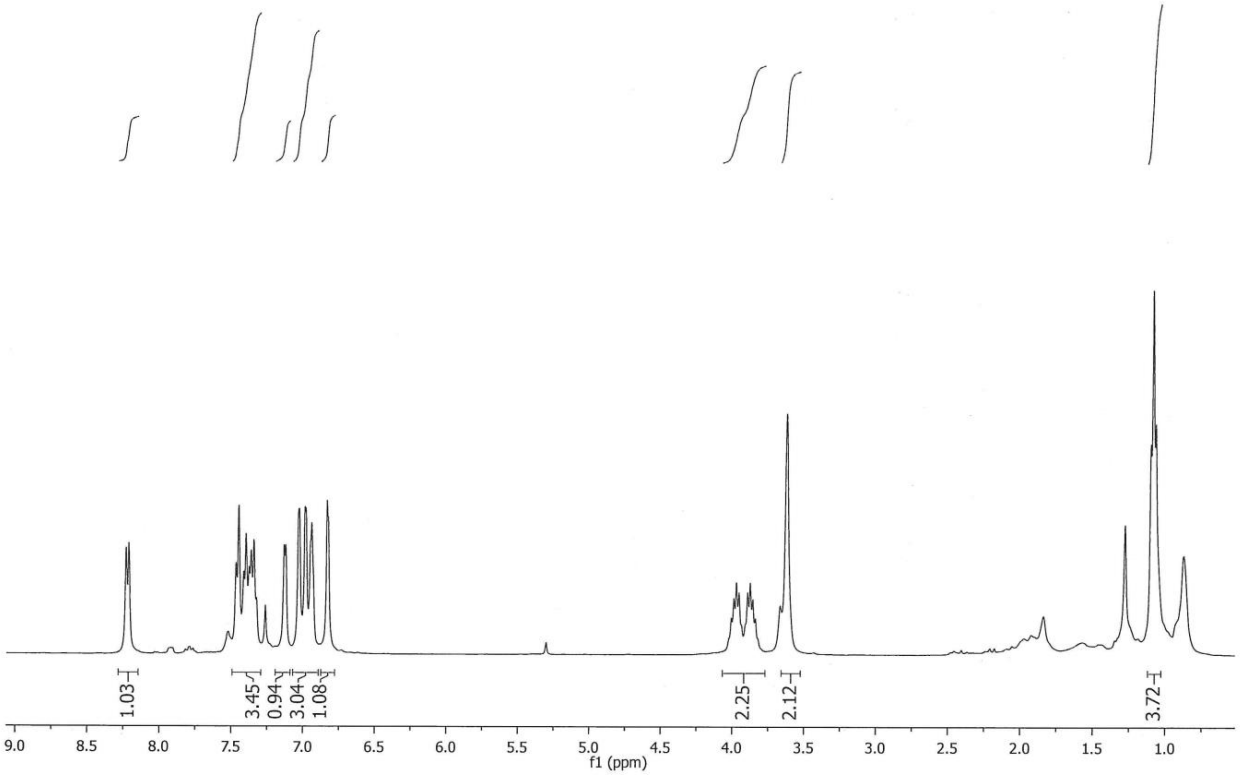

SI.3.12: ^{13}C NMR spectrum of IND-CH_2CH_3

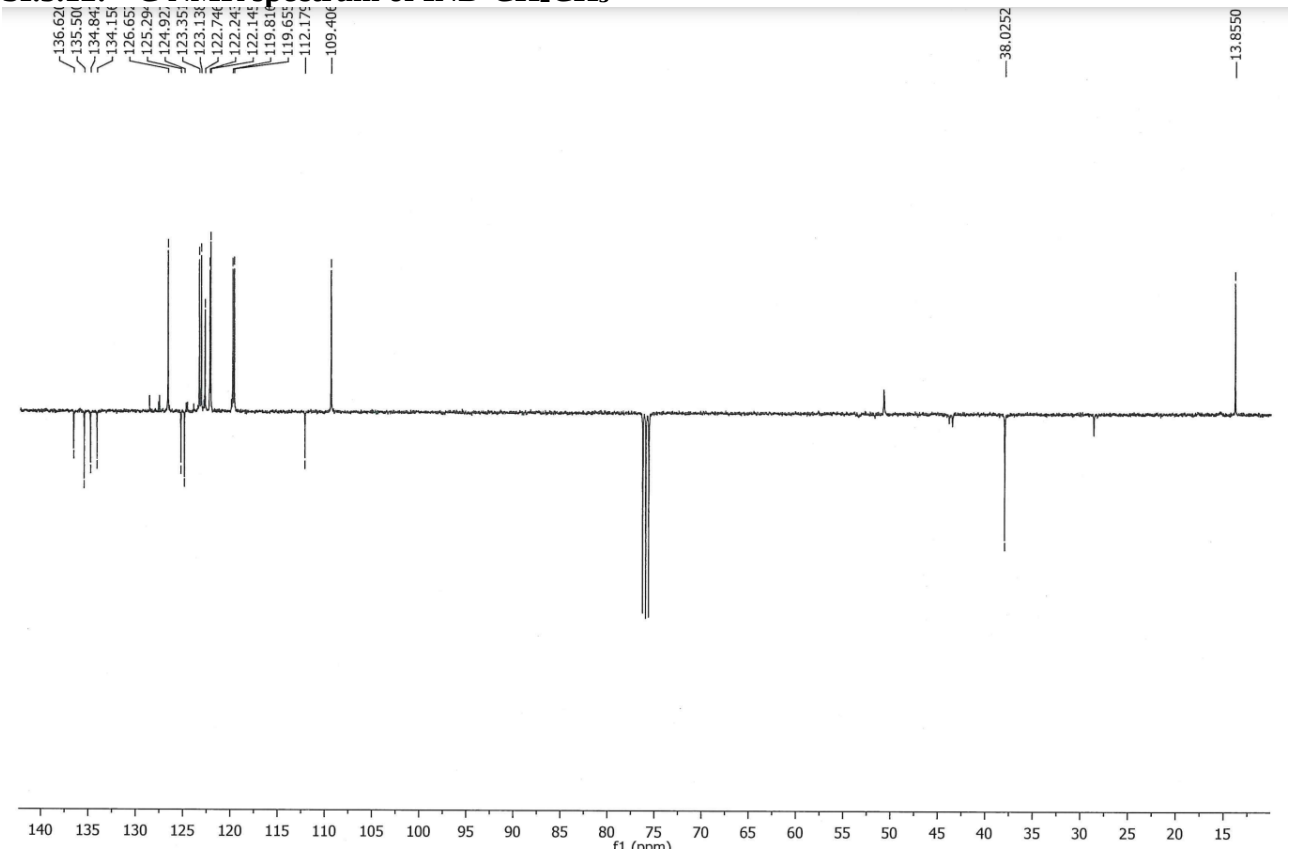

SI.4 Experimental setups for Electrochemical and Spectroelectrochemical experiments

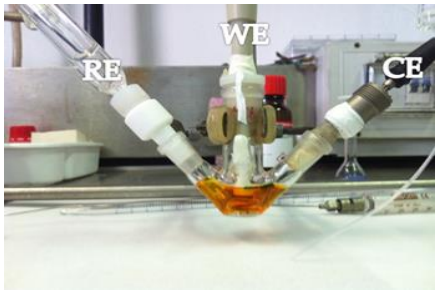

Fig. SI.4.1 Electrochemical minicell for voltammetry experiments. RE: reference electrode, WE: working electrode, CE: counter electrode.

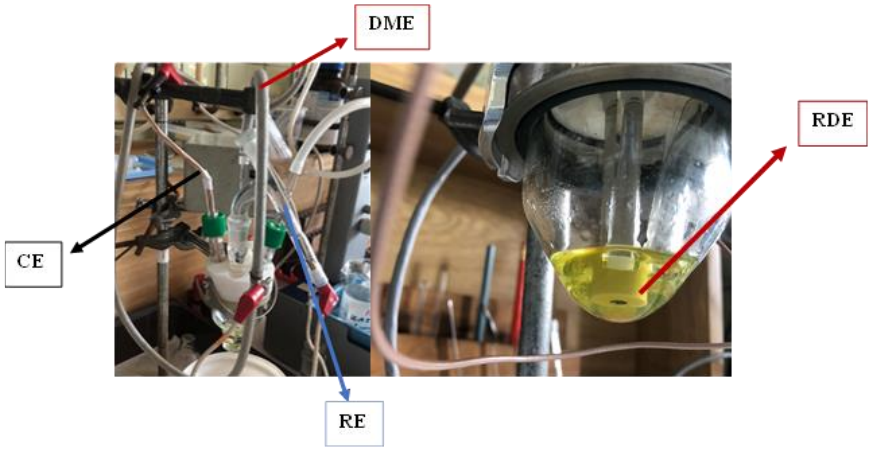

Fig. SI.4.2 Experimental setup for Dropping Mercury Electrode (DME) (left side) and Rotating Disk Electrode (RDE).

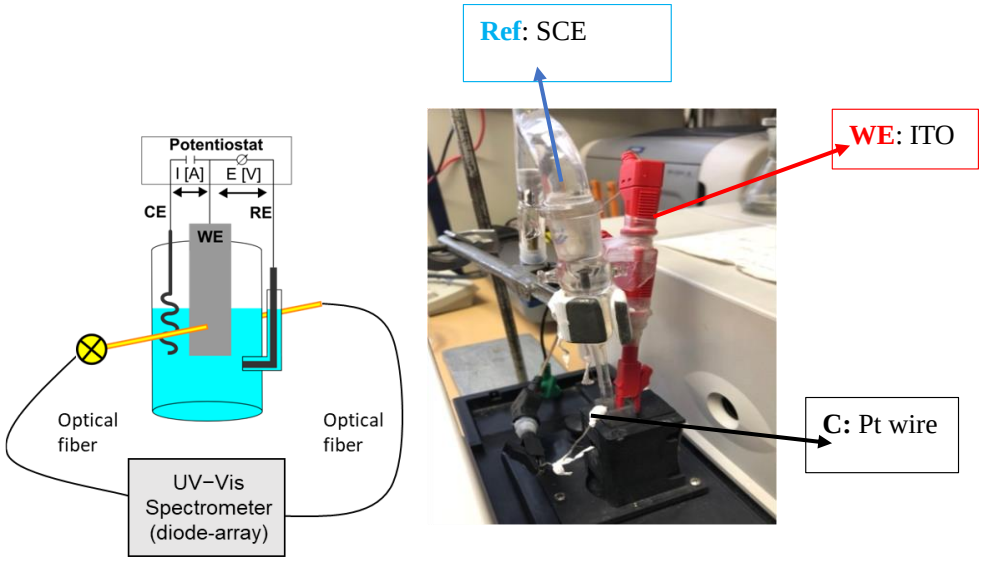

Fig. SI.4.3 Left side: scheme of the experimental set up employed for *in situ* thin film spectroelectrochemistry measurement. Right side: picture of the spectroelectrochemical cell, with electrode connections.

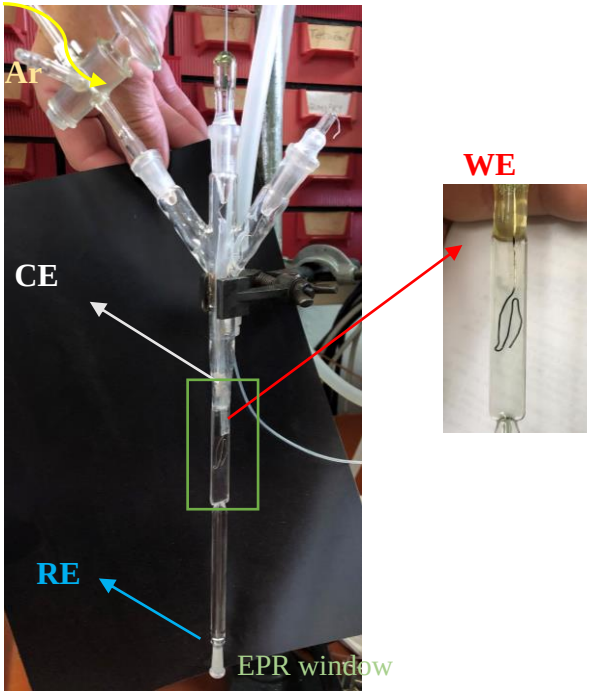

Fig. SI.4.4 EPR setup

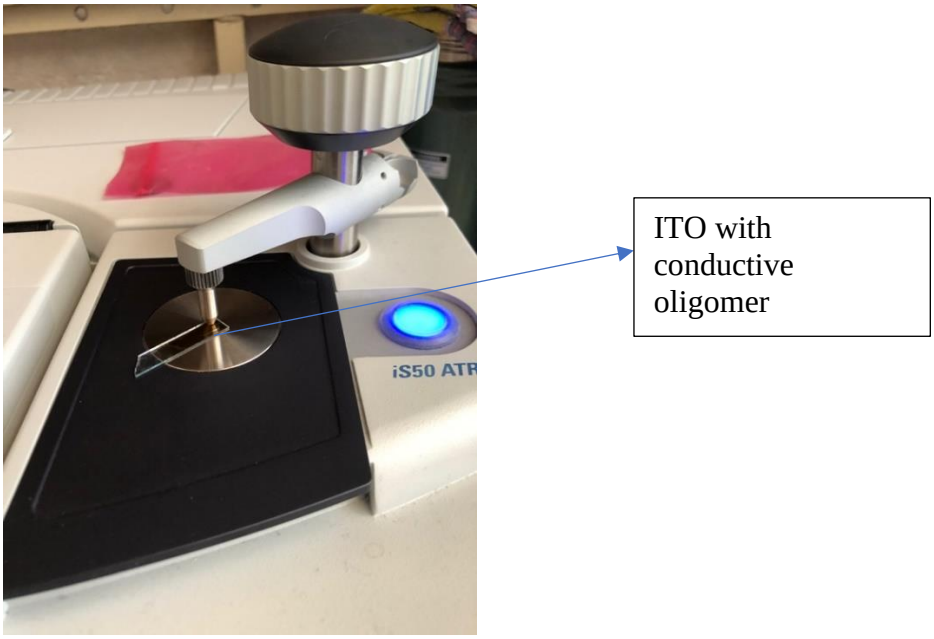

Fig. SI.4.5 ATR setup

SI.5. A comparative investigation of monomer solutions on different electrodes

	Solvent	E_{Ipc} *vs* Fc^+|Fc / V	E_{Ipa} *vs* Fc^+|Fc / V	$E_{LUMO, EC}$ / eV	$E_{HOMO, EC}$ / eV	$E_{HOMO-LUMO, EC}$ / eV
IND-CH_3	CH_2Cl_2	n.d.	0.39,0.57 0.81,0.92	n.d.	-5.19	n.d.
	CH_3CN	-2.75	0.44 0.79	-2.05	-5.24	3.19
IND-CH_2CH_3	CH_2Cl_2	n.d.	0.35,0.57 0.80	n.d.	-5.16	n.d.
	CH_3CN	-2.74	0.45 0.80,1.14	-2.74	-5.26	3.20
IND-$CH_2CH_3OCH_3$	CH_2Cl_2	n.d.	0.38,0.59 0.82,1.01	n.d.	-5.17	n.d.
	CH_3CN	-2.48	0.44 0.83, 1.15	-2.32	-5.26	2.94
IND-CH_2CH_3OH	CH_2Cl_2	n.d.	0.44,0.57 0.81	n.d.	-5.24	n.d.
	CH_3CN	-2.59	0.47 0.75,1.18	-2.21	-5.18	2.97

Table SI 5.1. A synopsis of CV results for the biindole monomers. First reduction and first oxidation peak potentials, normalized vs the Fc^+|Fc couple, from cyclic voltammetry on glassy carbon GC electrode (at 0.2 V/s scan rate), with corresponding estimated LUMO and HOMO energies and HOMO-LUMO energy gaps. $E_{LUMO(HOMO)}$ levels are calculated from CV data as 1e x [($E_{p,Ic(Ia)}$ /V (Fc^+|Fc) + 4.8 V (Fc^+|Fc *vs* zero)], consistent with Refs [12,13] in the main paper.

OXIDATION in ACN on GC		$E_{p,\,Ia}$	$E^0_1(E^{1/2})$	$E_{p,IIa}$	$E^0_2(E^{1/2})$	$E_{p,IIIa}$	$E^0_3(E^{1/2})$
		E_{Ipa} *vs* $Fc^+\|Fc$ / V		E_{IIpa} *vs* $Fc^+\|Fc$ / V		E_{IIIpa} *vs* $Fc^+\|Fc$ / V	
IND-CH_3	CV	0.44		0.79		1.12	
	RDE		0.41		0.75		0.95
IND-$CH_2CH_2OCH_3$	CV	0.44		0.81		1.15	
	RDE		0.43		0.79		0.98
IND-CH_2CH_2OH	CV	0.47		0.75		1.18	
	RDE		0.42		0.73		1.1
2,2′-bithiophene	CV			0.89		1.36	
	RDE				0.86		1.16

REDUCTION in MeCN				$E_{p,IIa}$		$E_{p,IIIa}$	
		E_{IpC} *vs* $Fc^+\|Fc$ / V	$E^0_1(E^{1/2})$	E_{IIpC} *vs* $Fc^+\|Fc$ / V	$E^0_2(E^{1/2})$	E_{IIIpC} *vs* $Fc^+\|Fc$ / V	$E^0_3(E^{1/2})$
IND-CH_3	GC	-2.64		-2.73		-2.96	
	RDE		-2.62		-2.69		-2.95
	HDME	-2.65		-2.74		-2.99	
	DME		-2.60		-2.69		-2.94
IND-$CH_2CH_2OCH_3$	GC	-2.66		-2.74		-2.99	
	RDE		-2.62		-2.71		-2.94
	HDME	-2.66		-2.73		-3.04	
	DME		-2.63		-2.71		n.d.
IND-CH_2CH_2OH	GC	-2.58		-2.68		-2.90	
	RDE		-2.59		-2.67		-2.87
	HDME	-2.59		-2.69		-2.91	
	DME		-2.56		-2.66		-2.87
2,2′-bithiophene	GC					-2.88	
	RDE						-2.84
	HDME					-2.88	
	DME						-2.82

Table SI.5.2. A comparative investigation of monomer solutions in MeCN with different techniques and different working electrodes (oxidation: cyclic voltammetry on GC, voltammetry in stationary conditions on RDE; reductions: cyclic voltammetry on GC and HDME, voltammetry in stationary conditions on RDE and DME) .

Estimation of HOMO and LUMO energy levels from voltammetric potentials.

LUMO and HOMO energy levels were estimated from the values of first reduction and first oxidation CV peak potentials in the working acetonitrile solvent, respectively, employing the following equation:

$$E_{LUMO(HOMO)} \text{ / eV} = -\,e \times [(E_{p,Ic(Ia)} \text{ / V } (Fc^+|Fc) + 4.8 \text{ V } (Fc^+|Fc \text{ vs zero})]$$

Where

$E_{LUMO(HOMO)}$ = estimated energy level of the LUMO (or HOMO) orbital (respect to the energy of an electron at rest in vacuum, in eV [S. Trasatti, *J. Electroanal. Chem.* **1986**, *209*, 417-428.]

e = electron (elementary charge; by expressing it in Coulomb instead, one would translate the energy from the eV scale to the joule scale (1 eV ~ $1.6 \cdot 10^{-19}$ joule))

$E_{p,Ic(Ia)}$ = first reduction (or first oxidation) CV peak potential (in Volt) in the working acetonitrile solvent for the investigated molecule, referred to the formal potential of the $Fc|Fc^+$ redox couple in the same working conditions

4.8 V = approximate estimated value for the absolute potential of $Fc^+|Fc$ in acetonitrile, consistent with the treatment by A. A. Isse, A. Gennaro, *J. Phys. Chem. B* **2010**, *114*, 7894-7899, according to which

$$E^{0,\mathrm{SCE\ aq}}_{\mathrm{O|R,S}} = E^{0,\mathrm{abs}}_{\mathrm{O|R,S}} - E^{\mathrm{abs}}_{\mathrm{SCE,aq}} + E_L = E^{0,\mathrm{abs}}_{\mathrm{O|R,S}} - E^{\mathrm{abs}}_{\mathrm{H+|H2,aq}} - 0.241 + E_L$$
$$= E^{0,\mathrm{abs}}_{\mathrm{O|R,S}} - 4.281 - 0.241 + E_L = E^{0,\mathrm{abs}}_{\mathrm{O|R,S}} - 4.522 + E_L$$
$$= E^{0,\mathrm{abs}}_{\mathrm{O|R,S}} - 4.522 + 0.093$$

(with 0.093 V being an estimated value for the intersolvental liquid juction potential E_L between the saturated aqueous calomel electrode and a 0.1 M tetraalkylammonium supporting electrolyte in acetonitrile [Diggle, J. W.; Parker, A. J. *Aust. J. Chem.* **1974**, *27*, 1617, cited in the above Isse and Gennaro paper])

Applying such expression to the case of the $Fc^+|Fc$ redox couple, for which our formal potential typically measured in acetonitrile vs the SCE is ~0.390 V, we get:

$E^{0,\mathrm{abs}}_{\mathrm{Fc+|Fc,S}} = E^{0,\mathrm{SCE\ aq}}_{\mathrm{Fc+|Fc,S}} + E^{\mathrm{abs}}_{\mathrm{SCE,aq}} - E_L$ = 0.390 + 4.522 − 0.093 = 4.82 V (rounding to the second digit).

Such value is also nearly coincident with the 4.93±0.10 V value proposed in a theoretical recent paper [M.Z. Makós, P. K. Gurunathan, S. Raugei, K. Kowalski, V.-A. Glezakou, R. Rousseau, *J. Phys. Chem. Lett.* 2022, 13, 42, 10005–10010]. In any case, it is an estimated value for which an uncertainty of one or a few units should be taken into account on the first decimal digit; but for our aim it is quite sufficient.

SI.6 *In-situ* EPR spectroelectrochemistry of IND-CH_2CH_3

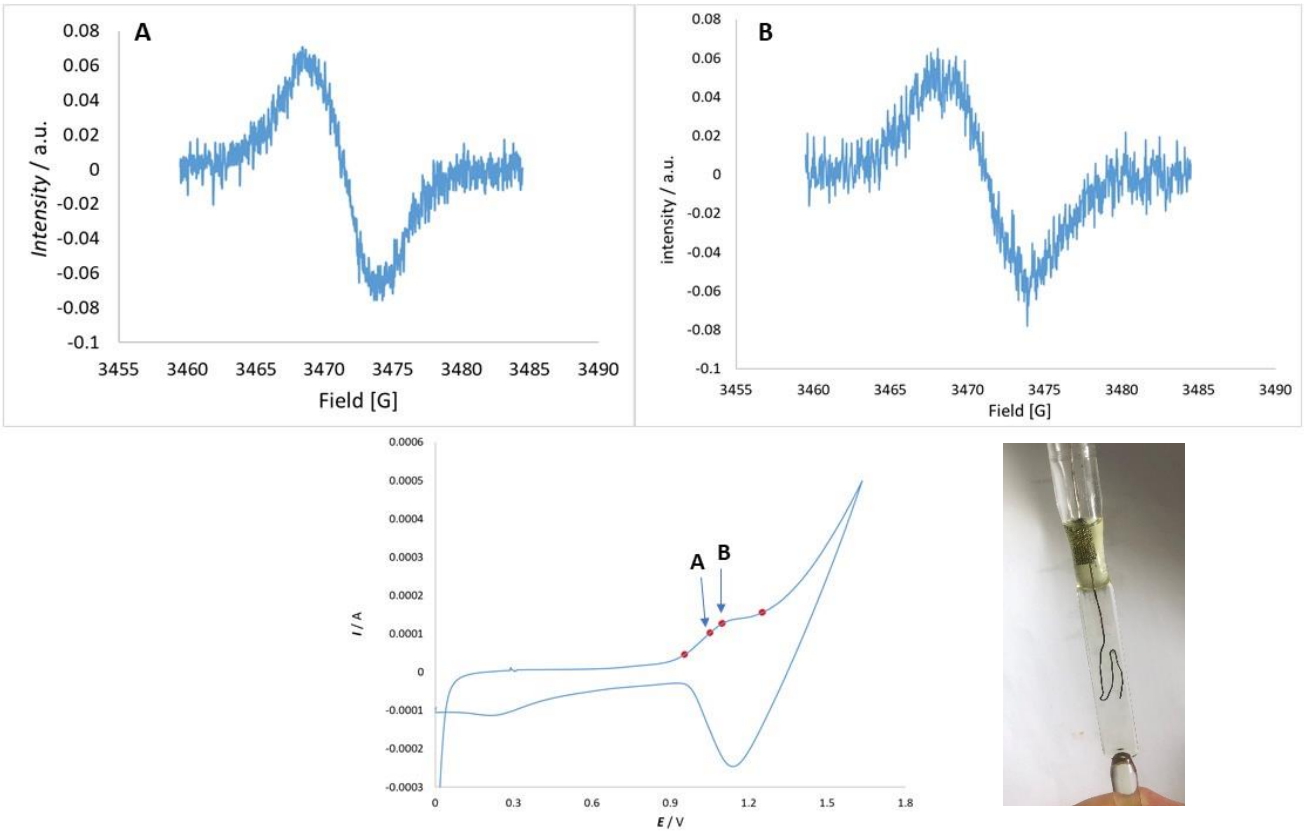

Figure SI.6.1 *In-situ* EPR spectroelectrochemistry patterns recorded for **IND-CH_2CH_3**. Potentials are referred to the Ag pseudoreference electrode.

SI.7 In-situ UV-Vis spectroelectrochemistry of IND-$CH_2CH_2OCH_3$ and IND-CH_3

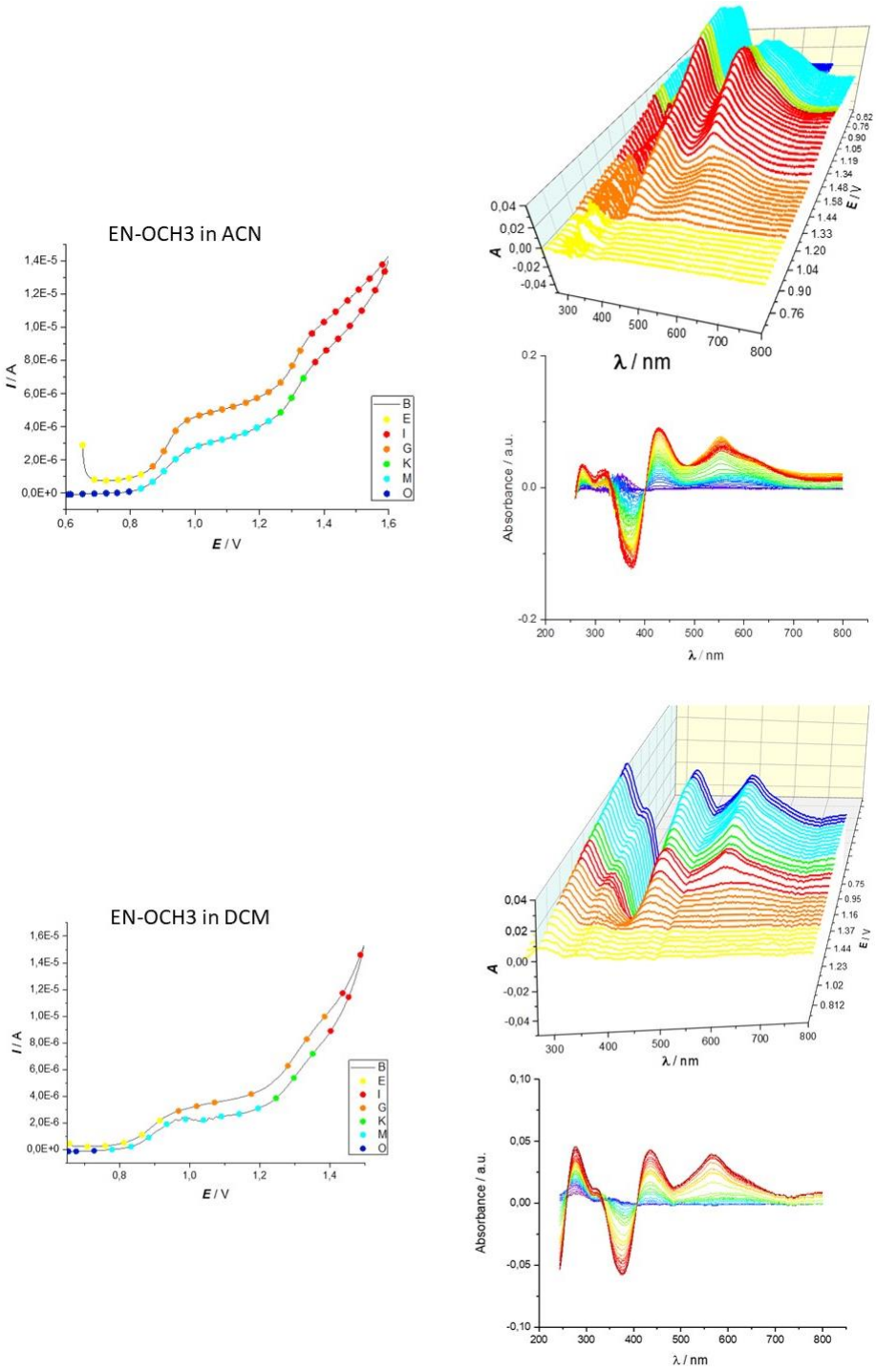

Figure SI.7.1 UV-vis spectroelectrochemistry of **IND-$CH_2CH_2OCH_3$**: 3D and 2D differential absorbance plots with related CV pattern, in CH_2Cl_2 (top) and CH_3CN (top).

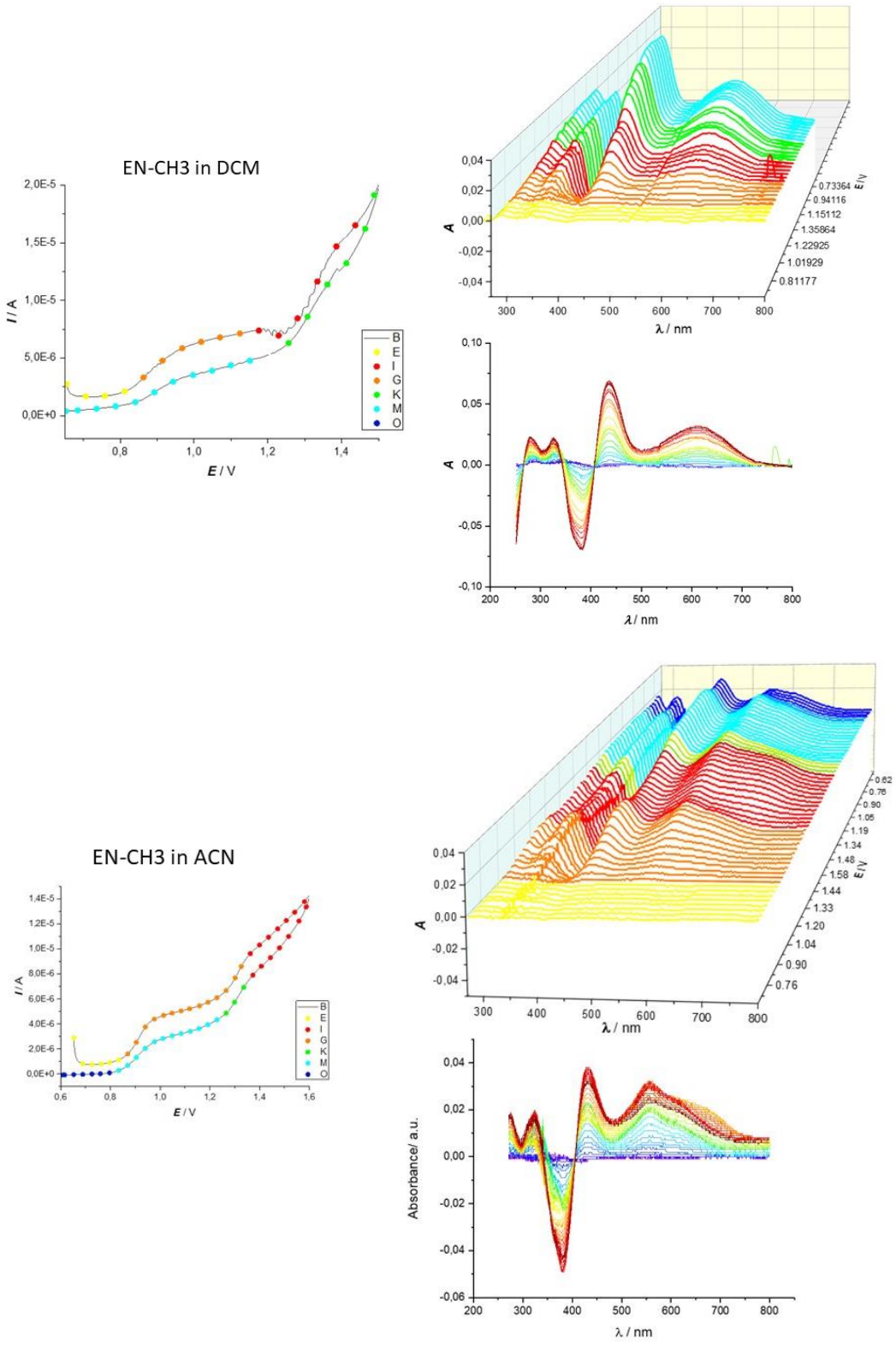

Figure SI.7.2 UV-vis spectroelectrochemistry of **IND-CH$_3$**: 3D and 2D differential absorbance plots with related CV pattern, in CH_2Cl_2 (top) and CH_3CN (top).

SI.8 UV-Vis-NIR spectroelectrochemistry of oligo-IND-$CH_2CH_2OCH_3$ and oligo-IND-CH_3 films

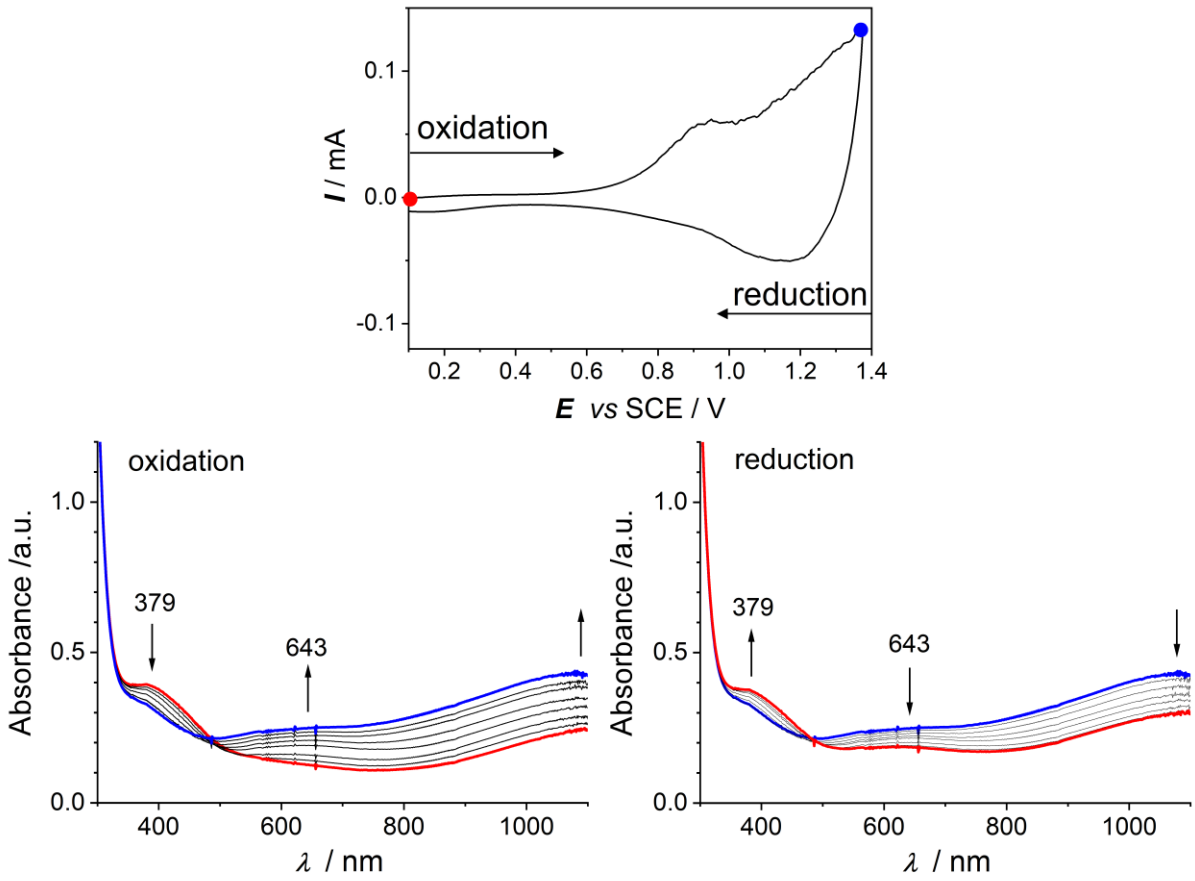

Figure SI.8.1. UV-Vis-NIR spectroelectrochemistry of **oligo-IND-$CH_2CH_2OCH_3$** film electrodeposited by 30 oxidation cycles on ITO electrode. Top: Cyclic voltammogram of the film recorded at 20 mV/s in 0.1 M $TBAPF_6$ and CH_2Cl_2 supporting electrolyte. Bottom: In-situ UV-Vis-NIR spectrum taken every 2 s during the oxidation (left) and back reduction (right) CV scan.

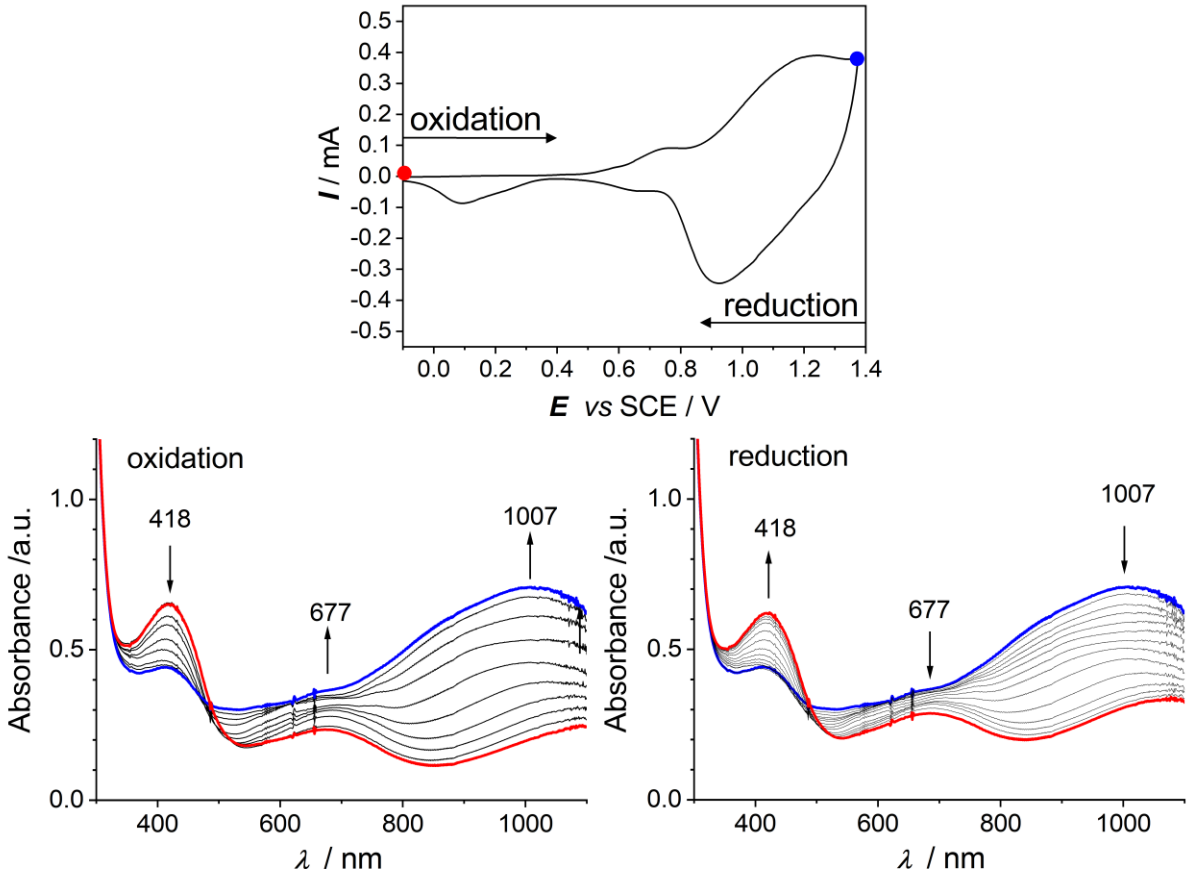

Figure SI.8.2. UV-Vis-NIR spectroelectrochemistry of **oligo-IND-CH$_3$** film electrodeposited by 20 oxidation cycles on ITO electrode. Top: Cyclic voltammogram of the film recorded at 20 mV/s in 0.1 M $TBAPF_6$ and CH_2Cl_2 supporting electrolyte. Bottom: In-situ UV-Vis-NIR spectrum taken every 2 s during the oxidation (left) and back reduction (right) CV scan.

SI.9 CV patterns of chiral probes Naproxen, Ketoprofen and Ibuprofen in various media, and related Table with peak potential summary

a) Naproxen

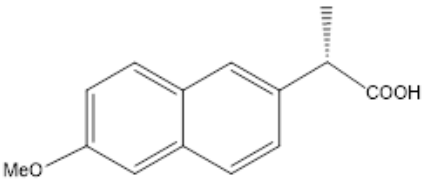

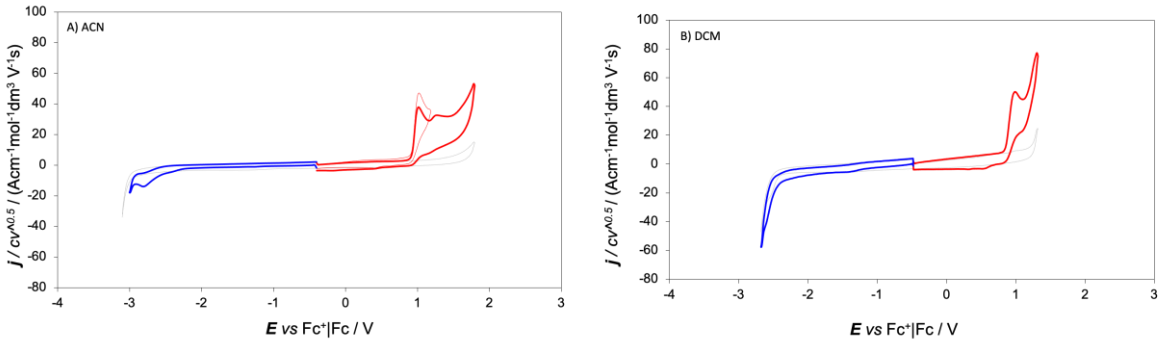

SI.9.1 Normalized CV patterns of (*S*)-Naproxen on GC electrode at 0.2 V s^{-1} scan rate in (a) MeCN and (b) CH_2Cl_2, in both cases with 0.1 M $TBAPF_6$ as supporting electrolyte.

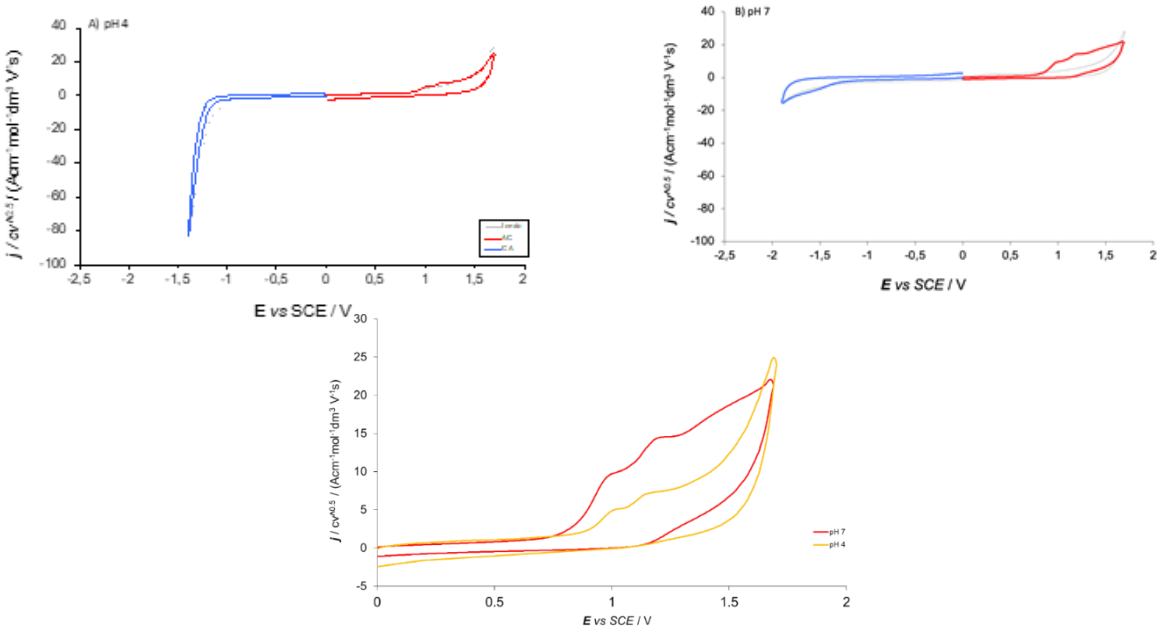

SI.9.2 CV patterns of (*S*)-Naproxen on GC electrode at 0.2 V s^{-1} scan rate in (a) pH 4 buffer and (b) pH 7 buffer. (c): comparison of the oxidation range at pH 4 and pH 7.

The increasing current trend with increasing pH was also found in a previous study ([25] in the main manuscript), although with no provided explanation. It is however worthwhile noticing that according to its pK_a ~4.2 ([37] in main manuscript) the molecule is practically only in anionic form at pH 7, while in comparable quantities of the undissociated and anionic form at pH 4. In any case, the pH 7 buffer was chosen as a convenient medium for the enantiodiscrimination tests.

b) Ketoprofen

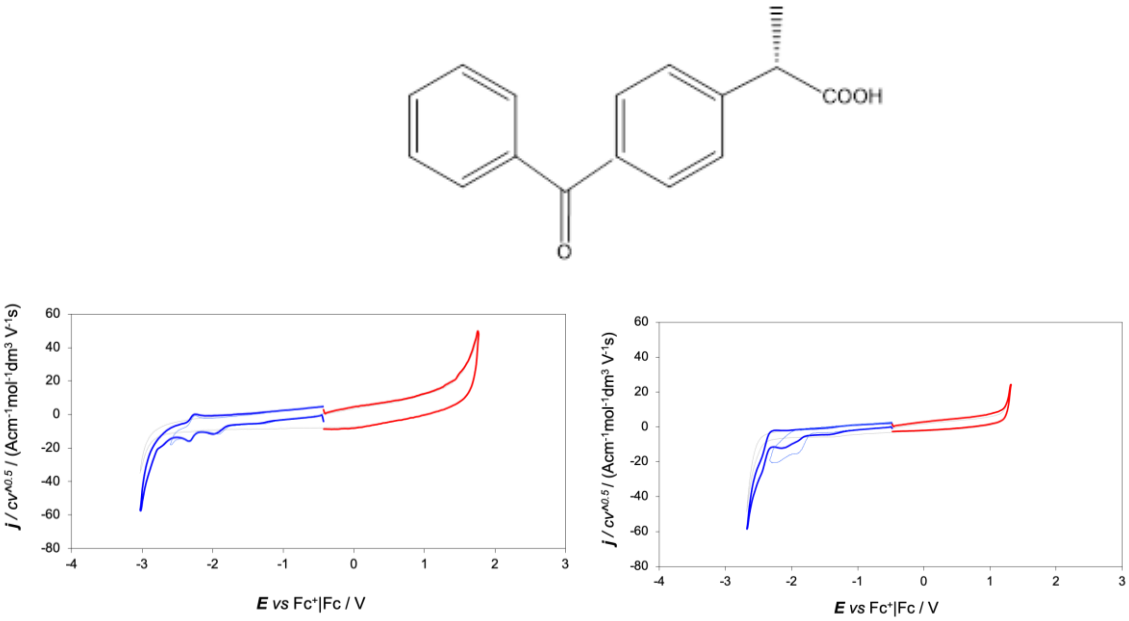

Figure SI.9.3. Normalized CV patterns of (*S*)-Ketoprofen on GC electrode at 0.2 V s^{-1} scan rate in (a) acetonitrile (ACN) e (b) dichloromethane (DCM), in both cases with 0.1 M $TBAPF_6$ as supporting electrolyte.

c) Ibuprofen

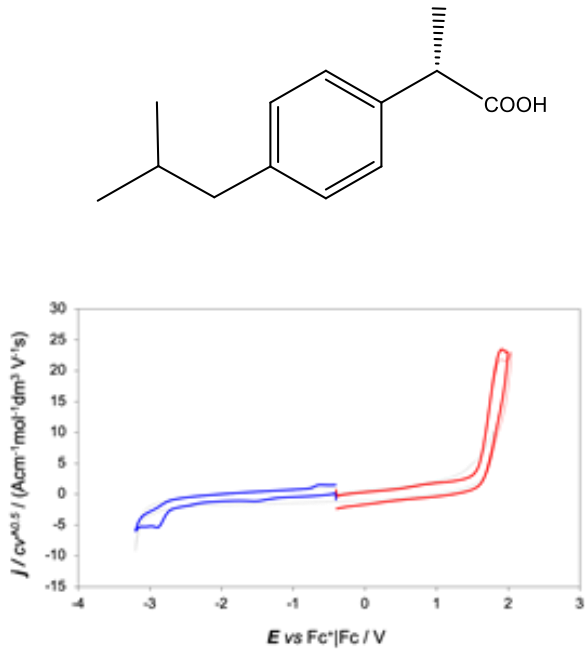

Figure SI.9.4. Normalized CV pattern of (*S*)-Ibuprofen on GC electrode at 0.2 V s^{-1} scan rate in acetonitrile (ACN) + 0.1 M $TBAPF_6$ as supporting electrolyte.

The reduction peak of Ibuprofen is probably due to reduction of the proton from the **COOH** group of the molecule while the oxidation at high potential value can be related to the formation of an aromatic radical cation.

Comparative Table of CV peak potentials for the three profens in different media

		E_{Ipa} *vs* $Fc^+|Fc$ / V	E_{Ipc} *vs* $Fc^+|Fc$ / V
Ketoprofen	DCM	n.d	-1.99
	ACN	n.d	-2.2
Naproxen	DCM	1.03	n.d.
	ACN	0.98	-2.79
	pH 4	1.0	n.d.
	pH 7	1.0	n.d.
Ibuprofen	ACN	1.94	-2.9

Table SI.9 A comparison of key voltammetric parameters of the three profens in four media (ACN and DCM with 0.1 M $TBAPF_6$ as supporting electrolyte, and aqueous pH 4 and pH 7 buffers).

SI.10 Comparison of enantiomer potential differences observed in enantiodiscrimination experiments by changing selector or probe in systematic sequences

SELECTORS	PROBES		$E_{p(S)}$-$E_{p(R)}$ / V
	(*R*)-Fc E_p/V	(*S*)-Fc E_p/V	
(*S*)-IND-CH_2CH_3	0.49	0.59	**0.10**
(*R*)-IND-$CH_2CH_2OCH_3$	0.63	0.43	**-0.20**
(*S*)-IND-CH_2CH_2OH	0.41	0.66	**0.25**

SELECTORS	PROBES		
	(*S*)-Naproxen E_p/V	(*S*)-Ketoprofen E_p/V	Enantyum® E_p/V
(*R*)-IND-CH_3	1.10		
(*S*)-IND-CH_3	1.23		
$E_{p(S)}$ -$E_{p(R)}$ / V	**0.13**		
(*R*)-IND-CH_2CH_3	1.10		
(*S*)-IND-CH_2CH_3	1.20		
$E_{p(S)}$ -$E_{p(R)}$ / V	**0.10**		
(*R*)-IND-$CH_2CH_2OCH_3$	1.11	-1.58	
(*S*)-IND-$CH_2CH_2OCH_3$	1.28	-1.70	
$E_{p(S)}$ -$E_{p(R)}$ / V	**0.17**	**0.12**	
(*R*)-IND-CH_2CH_2OH	0.91	-1.12	-0.70
(*S*)-IND-CH_2CH_2OH	1.37	-1.65	-1.56
$E_{p(S)}$ -$E_{p(R)}$ / V	**0.46**	**0.53**	**0.86**

SI.11 Reproducibility checks for enantiodiscrimination CV experiments

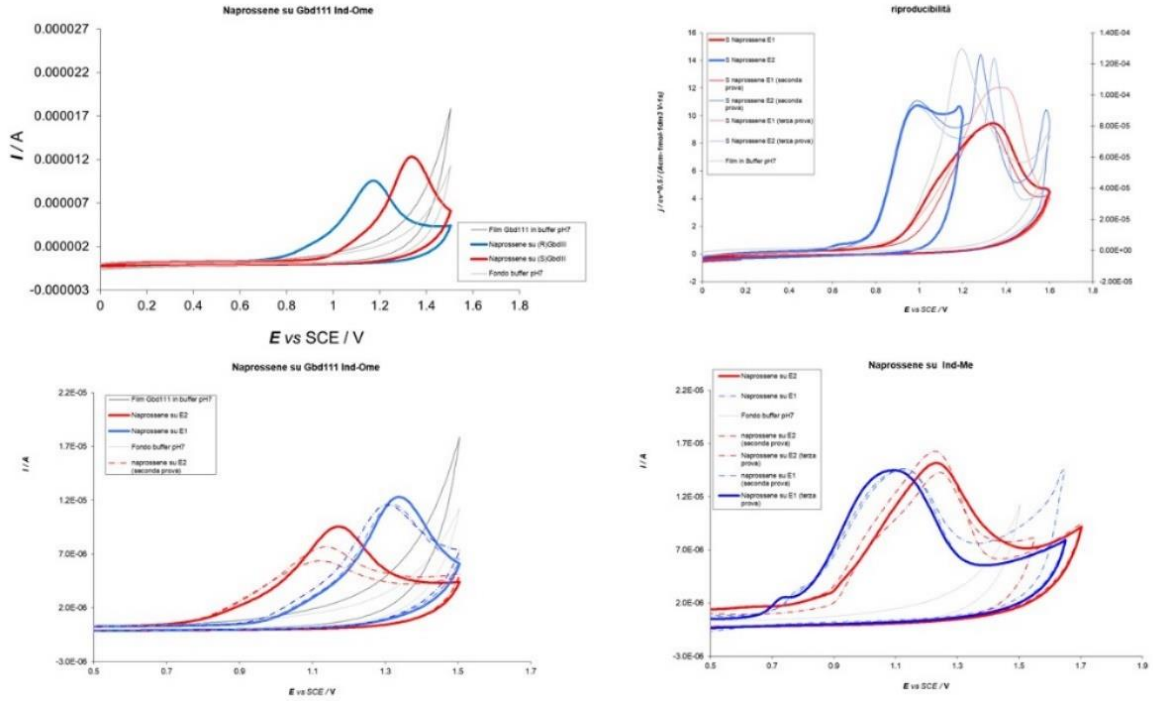

Figure SI.10.1 Reproducibility checks for Naproxen enantiodiscrimination CV experiments.

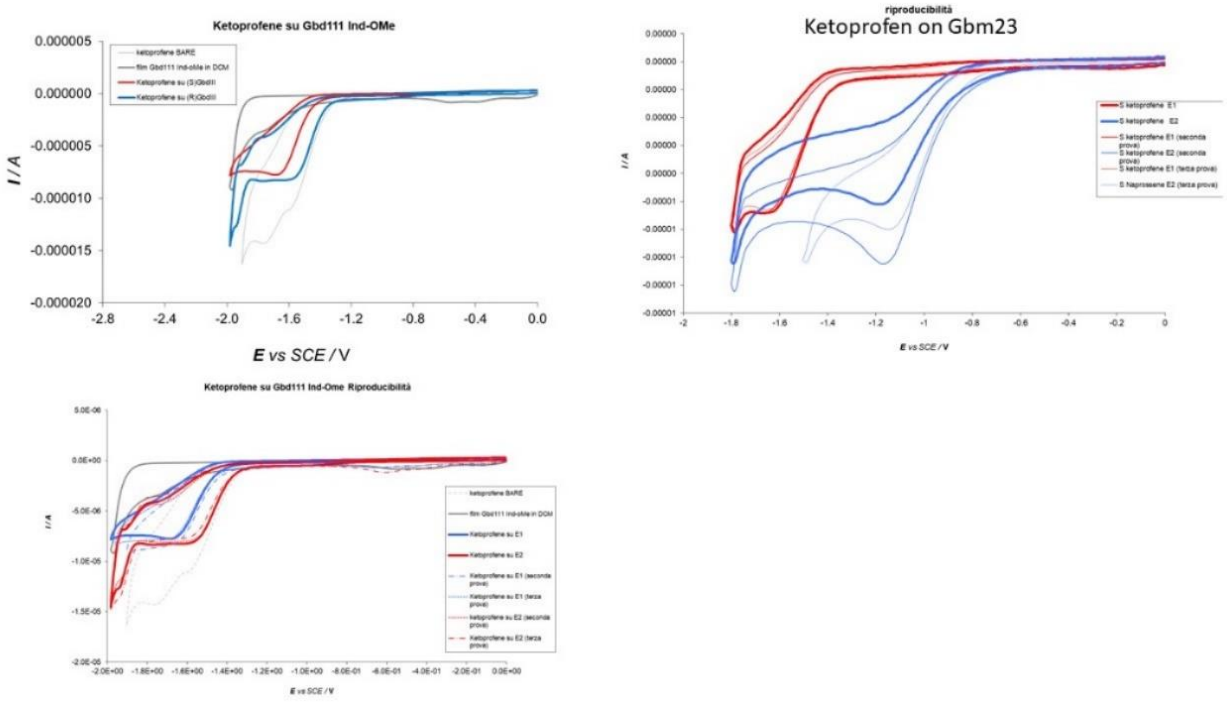

Figure SI.10.2 Reproducibility checks for Ketoprofen enantiodiscrimination CV experiments.